

This article has been downloaded from IOPscience. Please scroll down to see the full text article.

(<http://iopscience.iop.org/0953-8984/19/50/506206>)

More related content is available

Download details:

IP Address: 149.156.194.109

The article was downloaded on 20/12/2007 at 11:01

Please note that terms and conditions apply.

# Temperature dependence of magnetization under high fields in Re-based double perovskites

J M Michalik<sup>1,2</sup>, J M De Teresa<sup>1</sup>, J Blasco<sup>1</sup>, P A Algarabel<sup>1</sup>,  
M R Ibarra<sup>1,3</sup>, Cz Kapusta<sup>2</sup> and U Zeitler<sup>4</sup>

<sup>1</sup> Instituto de Ciencia de Materiales de Aragón, CSIC-Universidad de Zaragoza, 50009, Spain

<sup>2</sup> Department of Solid State Physics, Faculty of Physics and Applied Computer Sciences, AGH University of Science and Technology, 30-059 Cracow, Poland

<sup>3</sup> Instituto de Nanociencia de Aragón, Universidad de Zaragoza, Zaragoza, 50009, Spain

<sup>4</sup> High Field Magnet Laboratory, Institute for Molecules and Materials, Radboud University Nijmegen, 6525 ED Nijmegen, The Netherlands

Received 23 July 2007, in final form 25 October 2007

Published 19 November 2007

Online at [stacks.iop.org/JPhysCM/19/506206](http://stacks.iop.org/JPhysCM/19/506206)

## Abstract

We have carried out magnetization measurements in steady magnetic fields up to 30 T in ceramic samples of Re-based double perovskites ( $A_2\text{FeReO}_6$ ,  $A_2$  being  $\text{Ca}_2$ ,  $\text{Sr}_2$  and  $\text{BaSr}$ , and  $\text{Sr}_2\text{CrReO}_6$ ) in the temperature range from 4 to 300 K. These compounds show non-integer saturation magnetic moment due to the Re orbital contribution and are not completely saturated up to 30 T. The influence of magnetically disordered grain boundaries is revealed, and a model of approximation to saturation is given. The temperature dependence of various magnetic properties is described and compared among the samples.

(Some figures in this article are in colour only in the electronic version)

## 1. Introduction

Oxide half-metals, i.e. materials with only one spin direction present at the Fermi level either parallel or antiparallel to the magnetization direction, are being actively studied due to their potential applications in spin electronics [1]. Among them, ferromagnetic double perovskites have attracted a lot of interest due to their high Curie temperature ( $T_C$ ) and predicted half-metallicity [2, 3]. Re-based compounds are the most promising among the double perovskite family, exhibiting  $T_C$  as high as 520 K for  $\text{Ca}_2\text{FeReO}_6$  [4] or 610 K in the case of  $\text{Sr}_2\text{CrReO}_6$  [5], which is only surpassed by  $\text{Sr}_2\text{CrOsO}_6$  with  $T_C = 720$  K [6].

The  $A_2\text{FeReO}_6$  ( $A_2$  being  $\text{Ca}_2$ ,  $\text{Sr}_2$ ,  $\text{Ba}_2$ ) double perovskite compounds have already been studied in the past [7], and more recently in the context of new spintronic materials [8–15]. Their high  $T_C$  (305 K for  $A_2 = \text{Ba}_2$ , 410 K for  $A_2 = \text{Sr}_2$  and 520 K for  $A_2 = \text{Ca}_2$ ) was primarily explained on the basis of a spin-only model by the double-exchange like interaction between Fe and Re ions via the oxygen 2p orbital. However, a large Re orbital moment of the order of one-third of the Re spin moment was revealed by the x-ray magnetic dichroism (XMCD) [14], due to the strong spin-orbit coupling in the Re ions

(being 5d element) in  $A_2\text{FeReO}_6$  ( $A_2$  being  $\text{Ca}_2$ ,  $\text{CaSr}$ ,  $\text{Sr}_2$ ,  $\text{BaSr}$  and  $\text{Ba}_2$ ). The same study reveals that the orbital contribution to the magnetic moment of the Re ion drops (by 15% between  $\text{Ca}_2$  and  $\text{Ba}_2$ ) as the average ionic radius at the A site increases, showing a clear correlation with the lattice distortion. On the contrary, the total magnetic moment remains almost unchanged in series members. It was confirmed that the Re orbital moment plays an important role in the saturation magnetization of the Re-based double perovskites, making the spin-only model insufficient in order to describe the magnetic properties of these kind of compounds [16]. A strong ferromagnetic ordering leading to such high Curie temperatures, established by the electron hopping between Fe  $t_{2g}$  and Re  $t_{2g}$  orbitals via oxygen  $2p\pi$  ones should be strongly dependent on the lattice parameters. The lowering of the distances between the interacting ions reinforces the ferromagnetic state, while the deviation of the Fe–O–Re bond angle causes the hopping to be less efficient, and consequently weakens the magnetically ordered state. The interplay of the two processes should lead to an increase in  $T_C$  while changing the A ion from  $\text{Ba}_2$  to  $\text{Sr}_2$ , and finally to a decrease of the  $T_C$  for  $A_2 = \text{Ca}_2$ . One can see that the trend to increase the Curie temperature is different from the prediction of this simple model and some other process should be introduced to describe the  $T_C$  versus A ion size dependence. As discussed by Serrate *et al* [3] the hybridization of the oxygen orbitals opens the possibility of establishing a new interaction channel via the O  $2p\sigma$  orbitals for the  $e_g$  Fe and Re electrons. Besides, the electrical properties of the  $A_2\text{FeReO}_6$  series are not obvious. On the one hand, the room temperature resistivity is not influenced by the change of the cation size. However, the temperature dependence of the resistivity exhibits clear correlation with lattice changes [17]. The ground state changes from metallic for  $A_2 = \text{Ba}_2$  to semiconducting in the case of  $A_2 = \text{Ca}_2$  [4, 15]. The large value of the intergrain magnetoresistance found in these compounds led to the assumption of their half-metallicity [18, 19]. On the other hand, the magnetic state of the grain boundary was found to play an important role in the magnetoresistive properties of the ceramic polycrystalline  $(\text{Ba}_{0.8}\text{Sr}_{0.2})\text{FeMoO}_6$  compound due to intergrain magnetoresistance effects [20]. The ordering of the magnetic moments at the grain boundary was also studied by means of XMCD experiments in  $\text{Ca}_2\text{FeReO}_6$  samples by Azimote *et al* [21]. As will be shown later, the approach to the saturation of the magnetization behaviour is also strongly influenced by the magnetically disordered grain boundaries.

Similarly to the FeRe-based double perovskite compounds, XMCD measurements also show a significant Re orbital moment value for  $\text{Sr}_2\text{CrReO}_6$  (being, as in the former case, of the order of one-third of the spin moment value) [14, 22]. The *density functional theory* (DFT) calculations including the spin–orbit coupling [23, 24] predicted the saturation magnetization to be 30% larger than the previously assumed spin-only values. Our magnetic measurements confirmed the Re orbital moment to be important in the description of the magnetism of this double perovskite family member [25]. In  $\text{Sr}_2\text{CrReO}_6$  the crystal structure changes from cubic at room temperature to tetragonal at low temperatures with the transition temperature  $T_S \approx 260$  K [13].

In this paper we will show results of magnetization measurements under static magnetic fields up to 30 T. The contribution of the disordered grain boundaries to the approach to the saturation magnetization will be demonstrated, proving the need for such large fields in order to saturate the material. We will also present the temperature dependence of the magnetization in the temperature range from 4 K up to above the Curie temperature of each sample.

## 2. Sample preparation and characterization

We have chosen high-quality polycrystalline samples belonging to the  $A_2\text{FeReO}_6$  series ( $A_2$  being  $\text{Ca}_2$ ,  $\text{Sr}_2$  and  $\text{BaSr}$ ) and  $\text{Sr}_2\text{CrReO}_6$  sample to carry out the magnetic measurements. The

**Table 1.** Data on the crystallographic (space group and lattice parameters at room temperature, percentage of antisite defects) and magnetic (Curie temperature  $T_C$ , experimental magnetization value under 30 T at 4 K and coercive field) properties of the investigated Re-based compounds.

Compound	Space group	Lattice parameters	Antisites (%)	$T_C$ (K)	$M$ at 30 T and 4 K	
					( $\mu_B$ /f.u.)	$\mu_0 H_C$ at 4 K (T)
BaSrFeReO <sub>6</sub>	$Fm-3m$	$a = 7.9642(2) \text{ \AA}$	0.5	360	3.27	0.24(3)
Sr <sub>2</sub> FeReO <sub>6</sub>	$I4/m$	$a = 5.5613(1) \text{ \AA}$ $c = 7.9015(2) \text{ \AA}$	2	410	3.23	0.26(3)
Ca <sub>2</sub> FeReO <sub>6</sub>	$P2_1/n$	$a = 5.4029(1) \text{ \AA}$ $b = 5.5278(1) \text{ \AA}$ $c = 7.6865(1) \text{ \AA}$ beta = 90.055(3)	0	520	3.12	1.03(5)
Sr <sub>2</sub> CrReO <sub>6</sub>	$Fm-3m$	$a = 7.8152(1) \text{ \AA}$	13.5	610	1.01	1.29(5)

samples were synthesized by a solid-state reaction technique described elsewhere [13, 17]. The progress of the synthesis was controlled at each step by means of x-ray powder diffraction using the Rigaku D/MAX 300 diffractometer with a rotating anode and a wavelength of Cu  $K\alpha$ . The Rietveld refinements of the x-ray diffraction spectra performed with FULLPROF software [26] indicate that all samples are mainly of double perovskite phase with some small impurity traces. At room temperature the crystal structure is cubic ( $Fm-3m$  space group) for BaSrFeReO<sub>6</sub> and Sr<sub>2</sub>CrReO<sub>6</sub>, tetragonal ( $I4/m$ ) for Sr<sub>2</sub>FeReO<sub>6</sub>, and monoclinic ( $P2_1/n$ ), for Ca<sub>2</sub>FeReO<sub>6</sub>. Those structural differences can be understood taking into account the tiling of the Fe(Cr)/Re–O octahedra. While the A cation size is getting smaller, empty space shows up around it and needs to be filled up. The cubic structure is then replaced by the space groups exhibiting lower symmetry. Using Glazer's terminology [27] the  $a^0a^0c$  octahedral tilt is responsible for the occurrence of the  $I4/m$  space group, while the  $P2_1/n$  space group arises from the  $a^+b^-b^-$  tilt. Those tilts shift the oxygen atoms from their ideal positions and give rise to the additional diffraction peaks. Moreover, the Ca<sub>2</sub>FeReO<sub>6</sub> sample shows a structural transition (between two monoclinic phases) at about 140 K [10, 11, 15], which has a significant impact on various properties [10–12, 15]. The level of antisite disorder (AS) defects, estimated by the x-ray pattern analysis (see [16]) was very low for the Fe-based samples. Here we define the percentage of AS defects in such a way that 0% indicates a fully ordered defect-free structure and 50% means a fully disordered sample, i.e. the single perovskite phase instead of the double perovskite one. As proposed by Balcells *et al* [28] the saturation magnetization ( $M_S$ ) decreases linearly in Sr<sub>2</sub>FeMoO<sub>6</sub> from its highest value for AS = 0% down to  $M_S = 0$  for AS = 50%. In our samples the amount of AS is only 0% for Ca<sub>2</sub>FeReO<sub>6</sub>, 0.5% for BaSrFeReO<sub>6</sub> and 2% for Sr<sub>2</sub>FeReO<sub>6</sub> (see also table 1). This allows investigation of the magnetization in good-quality samples without the need for significant corrections due to structural defects, leading to clear interpretation of the results. The room temperature x-ray diffraction pattern for the Ca<sub>2</sub>FeReO<sub>6</sub> is presented in figure 1, and the simulated patterns for different levels of AS disorder (0% and 5%) are presented in its inset.

The presence of magnetic impurities can produce spurious signals in the study of magnetic properties. In order to discard such influences, samples have been carefully examined. The magnetization studies in the temperature range 300–700 K have been performed by means of an ADE Electronics EV7 vibrating sample magnetometer with the sensitivity of  $10^{-6}$  emu.  $T_C$  is found to be  $\approx 360$  K,  $\approx 410$  K and  $\approx 520$  K for BaSrFeReO<sub>6</sub>, Sr<sub>2</sub>FeReO<sub>6</sub> and Ca<sub>2</sub>FeReO<sub>6</sub>, respectively (see figure 2). The amount of magnetic impurities was estimated by the extrapolation of the linear (paramagnetic) part of the magnetization curve onto the ordinate

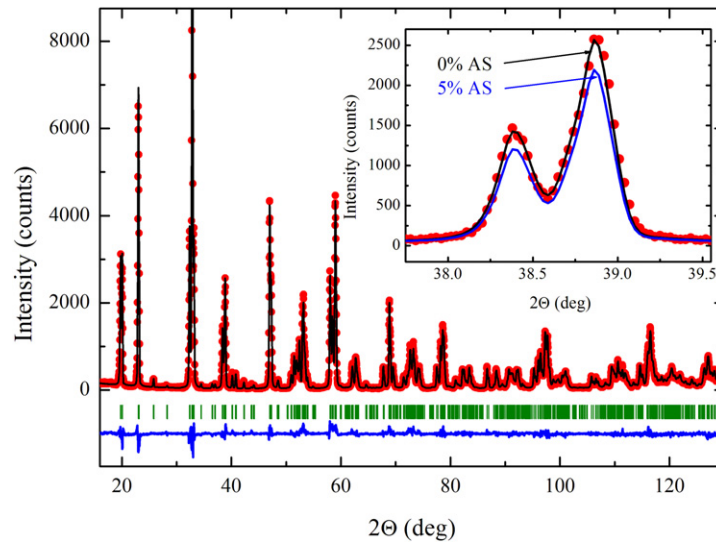


**Figure 1.** Room temperature x-ray diffraction pattern (circles) of the  $\text{Ca}_2\text{FeReO}_6$  sample and its Rietveld refinement (line). Ticks indicate the positions of the theoretical diffraction peaks according to the crystallographic structure, and the bottom line is the difference between the measured and theoretical intensity. The reliability factors are  $R_{\text{Bragg}} = 4.7\%$  and  $R_{\text{wp}} = 9.7\%$ . Inset: the data range from  $37.7^\circ$  to  $39.5^\circ$ . Circles indicate the experimental data, and the lines are the Rietveld refinement results for given levels of AS disorder.

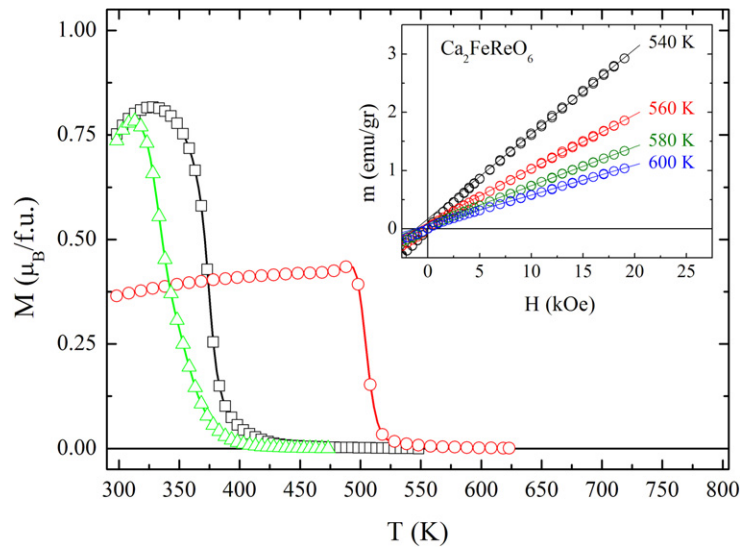


**Figure 2.** Magnetization under an applied field of 1 kOe versus temperature. Open circles, squares and triangles correspond to  $\text{Ca}_2\text{FeReO}_6$ ,  $\text{Sr}_2\text{FeReO}_6$  and  $\text{BaSrFeReO}_6$  samples, respectively. Inset: the magnetization curves at several temperatures in the paramagnetic region (over 520 K) for the  $\text{Ca}_2\text{FeReO}_6$  sample (circles), and a linear fit of the paramagnetic signal (lines) used to estimate the number of the magnetic impurities (see text for details).

axis (see inset of figure 2). The extrinsic magnetization caused by the impurities is estimated to be  $\approx 0.065 \text{ emu g}^{-1}$ ,  $\approx 0.25 \text{ emu g}^{-1}$  and  $\approx 0.05 \text{ emu g}^{-1}$  for  $\text{BaSrFeReO}_6$ ,  $\text{Sr}_2\text{FeReO}_6$  and

$\text{Ca}_2\text{FeReO}_6$ , respectively. Those values correspond to 0.2%, 0.7% and 0.1% of the saturation magnetization value measured for  $\text{BaSrFeReO}_6$ ,  $\text{Sr}_2\text{FeReO}_6$  and  $\text{Ca}_2\text{FeReO}_6$ , respectively.

In  $\text{Sr}_2\text{CrReO}_6$  the AS percentage is higher (AS = 13.5%) than in the  $\text{A}_2\text{FeReO}_6$  series due to the similar ionic size for  $\text{Cr}^{3+}$  (0.615 Å) and  $\text{Re}^{5+}$  (0.58 Å) ions [29]. The  $T_C$  of the  $\text{Sr}_2\text{CrReO}_6$  sample is about 610 K. Magnetization isotherms above  $T_C$  in this sample show the expected linear paramagnetic dependence with the magnetic field, and from the extrapolation of the linear behaviour onto the ordinate axis the extrinsic magnetization caused by ferromagnetic impurities is estimated to be  $\approx 0.009 \text{ emu g}^{-1}$ , which corresponds to only 0.1% of the low-temperature magnetic saturation.

High-field magnetization measurements up to 30 T have been performed at the High Field Magnet Laboratory, Radboud University Nijmegen, The Netherlands. The use of Bitter coils bearing a current of up to 37 kA allows the attainment of such large static magnetic fields [30]. We remark that the use of static magnetic fields is preferred in this kind of investigation to the use of pulsed magnetic fields in order to avoid spurious signals arising from fast field variations. In our experiment, the static magnetic field is first stabilized and the magnetization is measured with the extraction method via two pick-up coils connected in series-opposition. A bulk Ni sample with similar volume to our samples has been used for calibration of the absolute value of the magnetization. We performed the experiment in temperatures ranging from 4 to 300 K. The low temperature data have already been described in our recent paper [16]. In the present paper we provide further insight into the physics of these compounds through the study of the temperature dependence of the magnetization.

### 3. Approach to magnetic saturation

The electric conductivity of the ceramic pellets of the double perovskite materials is controlled mainly by the influence of the highly resistive grain boundaries. It was proposed that the grain boundary magnetic state in  $(\text{Ba}_{0.8}\text{Sr}_{0.2})_2\text{FeMoO}_6$  is a spin-glass like state [20]. Such a statement was supported by the successful fit of the high-field magnetoresistance results through a magnetic saturation law with the functional form widely used in spin-glasses with a weak random anisotropy field [31, 32]. In the proposed model weak anisotropy means that the exchange field is stronger than the random anisotropy field. In such a case a local ferromagnetic magnetization changes its direction significantly only over a distance of a range of a correlation length ( $R_a^3$ ). Several theoretical approaches have been proposed for systems with weak random anisotropy (spin-glasses, correlated spin-glasses, ferromagnets with wandering axis etc) [33]. As it is not the aim of this paper to develop a new complex model of the magnetically disordered grain boundary state we will use the model that well describes experimental magnetoresistance curves. In sharp contrast to the transport properties in granular materials the overall magnetization is mainly influenced by the bulk magnetization, i.e. the inner part of the grain. However, the lack of saturation in applied fields as high as 30 T can be ascribed to a lack of ordering in the highly disordered grain boundary region. It was confirmed by the XMCD study of the local Fe magnetic moments [21] that the grain boundary (at least 5 nm deep) is magnetically harder than the grain core and this fact was ascribed to the elevated level of AS disorder at the grain boundary. Larger hardness of the grain boundary compared to the grain core was also proposed by De Teresa *et al* [17] on the basis of the magnetoresistance measurements.

To study the approach to saturation magnetization we have applied the model with the functional form  $M(H) = a(1 - \frac{b}{\sqrt{H}})$  to describe the magnetic behaviour of the grain boundaries. Here  $a$  has the units of magnetization and  $b$  is a constant depending on random

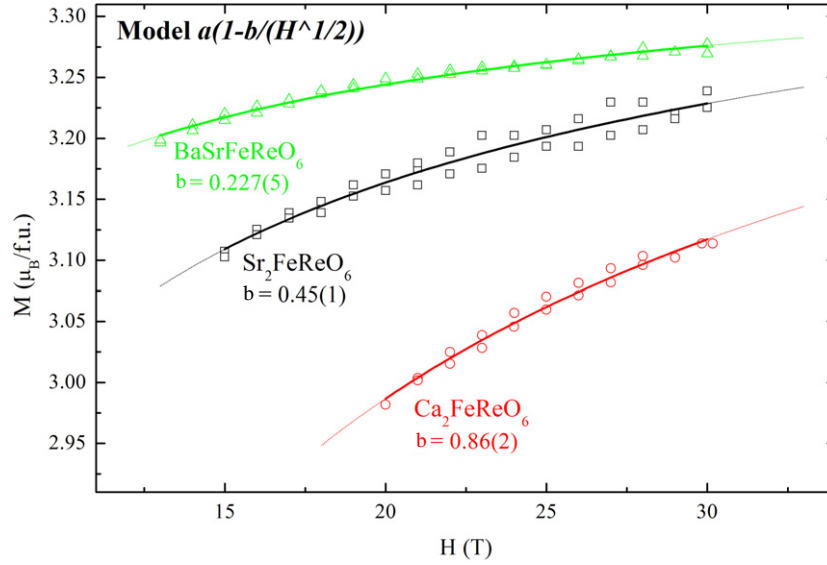


**Figure 3.** Fit of the magnetization data at 4.2 K with the model described in the text. Open circles, squares and triangles denote  $\text{Ca}_2\text{FeReO}_6$ ,  $\text{Sr}_2\text{FeReO}_6$  and  $\text{BaSrFeReO}_6$  samples, respectively. Dashed lines are obtained from fitting the model to the experimental data, and solid lines show the fitting range.

anisotropy ( $\beta_r^2$ ), the exchange strength ( $\alpha^{3/2}$ ) and the distance for which the local easy axes become uncorrelated ( $R_a^3$ ). The formal dependence on the abovementioned parameters is as follows:  $b = R_a^3 \frac{\beta_r^2}{15\alpha^{3/2}}$ . This model can be used in cases when the anisotropy is weaker than the exchange strength, and for magnetic fields smaller than the exchange field (the so-called low-field regime). The fitting of the model was performed in the range of several tesla from the maximum of 30 T, i.e. 10 T in the case of  $\text{Ca}_2\text{FeReO}_6$  (being the less saturated), and up to 16 T in the case of  $\text{BaSrFeReO}_6$  (an almost saturated sample). In figure 3 we present the experimental data along with the fitted model. The  $b$  parameter of the fit changes from 0.86(2) through 0.45(1) to 0.227(5) for  $\text{Ca}_2\text{FeReO}_6$ ,  $\text{Sr}_2\text{FeReO}_6$  and  $\text{BaSrFeReO}_6$ , respectively. We can discard the influence of the AS disorder as the explanation for such a wide range of  $b$  parameter values thanks to the high quality of the samples and a very low AS defect content. One can see that the definition of the  $b$  coefficient involves two competing properties—random anisotropy energy and the exchange strength. As the magnetic and magnetostriction measurements show [3, 8, 17], the increase in anisotropy that takes place when lowering the mean ionic radius at the A site could explain the evolution of the  $b$  parameter. Moreover, the XMCD data also indicate stronger orbital contribution as the mean radius of the alkali earth ions decreases [14]. As a consequence, it seems that a strong random anisotropy at the grain boundaries could be at the basis of the lack of magnetic saturation in these compounds.

The same model was applied to the  $\text{Sr}_2\text{CrReO}_6$  sample. The fitting procedure leads to the  $b$  parameter value of 0.19(2).

#### 4. Temperature dependence of the magnetization

The value of magnetization at a given temperature depends on the interplay amongst the applied magnetic field, the exchange interaction and the thermally excited spin-waves. The

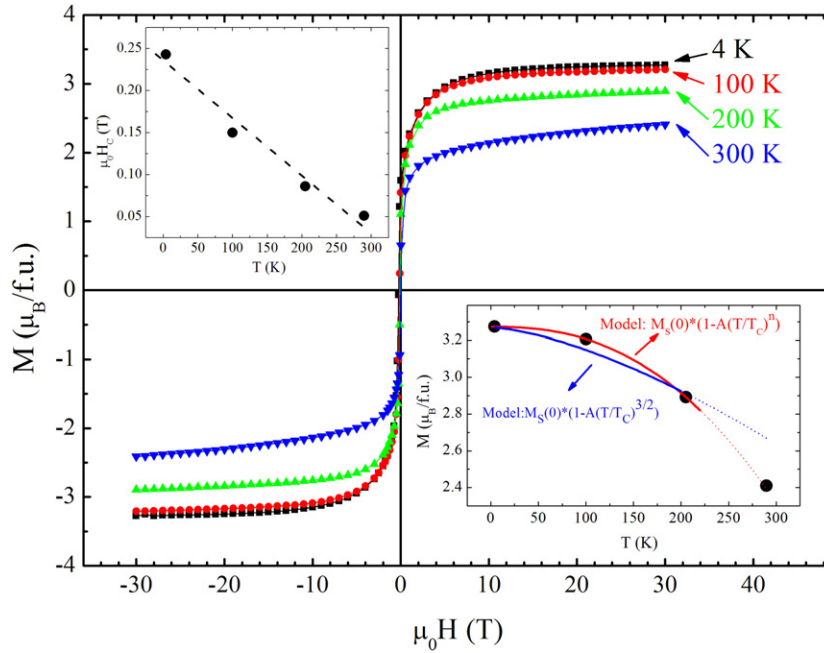


**Figure 4.** Magnetization curves at different temperatures (4, 100, 200 and 300 K) for BaSrFeReO<sub>6</sub>. Upper inset: coercive field dependence on the temperature (dashed line is a visual guideline). Lower inset: the evolution of saturation magnetization with temperature (circles), the fitting with the model described in text, and the curve obtained with the  $T^{3/2}$  Bloch law.

spin-wave concept was firstly proposed by Bloch [34] in the theorem giving the variation of the spontaneous magnetization as a function of the absolute temperature by the  $T^{3/2}$  law. This equation was further changed by adding the terms coming from the expansion of the function describing the spin-wave energy on the wavevector dependence. As a consequence the  $T^{5/2}$ ,  $T^{7/2}$  terms can be added [35].

The temperature dependence of the magnetization for BaSrFeReO<sub>6</sub> and Ca<sub>2</sub>FeReO<sub>6</sub> samples is presented in the lower inset of figure 4 and in figure 5(a), respectively. We have investigated this dependence using the Bloch model. This approach was only possible for the BaSrFeReO<sub>6</sub> sample due to several features exhibited by this particular sample. First of all the magnetization of this sample is the closest to the saturation magnetization, while in the case of the remaining Fe-based samples (Ca<sub>2</sub>FeReO<sub>6</sub> and Sr<sub>2</sub>FeReO<sub>6</sub>) the maximum value of magnetization obtained is still far from the saturation value. The structural transition in Ca<sub>2</sub>FeReO<sub>6</sub> also influences the values of the magnetization measured, making it impossible to use the Bloch model. The same situation happens in the case of the Sr<sub>2</sub>CrReO<sub>6</sub> sample.

The original  $T^{3/2}$  Bloch law does not give a satisfactory fit to our results in contrast to the results given by Lofland *et al* for the Sr<sub>2</sub>FeMoO<sub>6</sub> double perovskite (see [36]). On the other hand, the detailed analysis of the *nuclear magnetic resonance* (NMR) data done by Zajac *et al* (see [37]) reveals a  $T^{5/2}$  dependence of the Mo hyperfine field in this compound, as would be expected in half-metallic compounds [38]. Consequently, the model with the exponential parameter free and fixed saturation magnetization, i.e.  $M(T) = M(0)[1 - A_n(\frac{T}{T_c})^n]$ , was proposed [39]. Fitting leads to the value of  $n = 2.4$ , which is very close to the  $5/2$  exponent proposed for half-metals. The fit along with the experimental data is displayed in the lower inset of figure 4 and compared with the curve obtained from the original  $T^{3/2}$  Bloch law. The



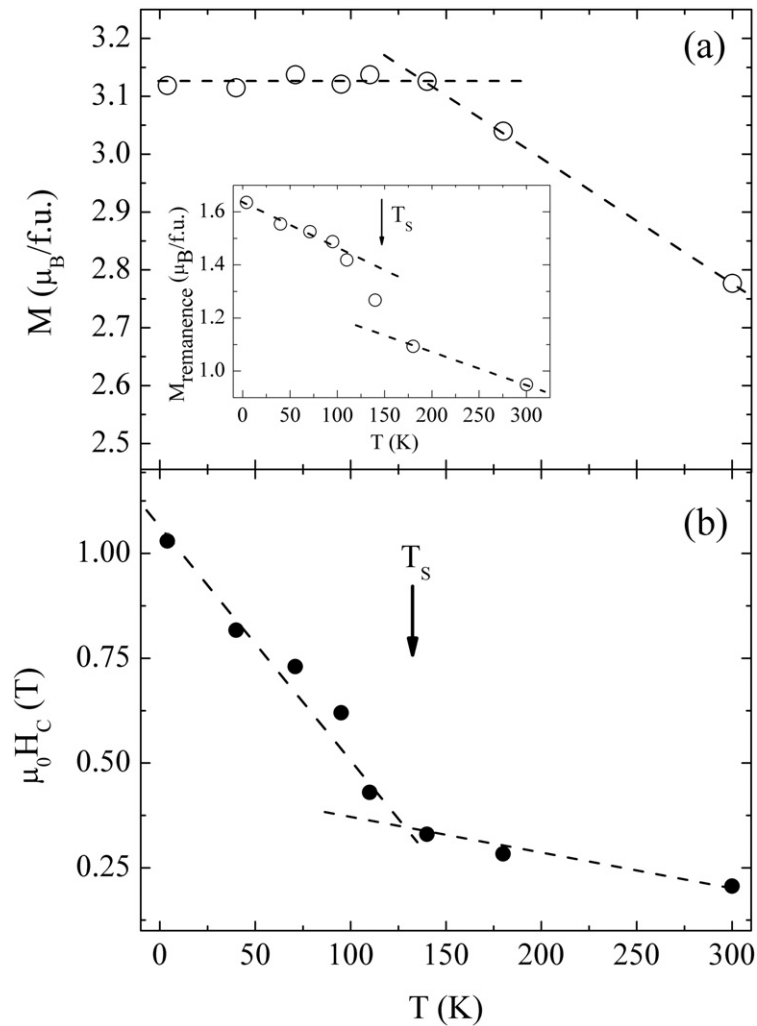


**Figure 5.** Magnetization under 30 T (a) and coercive field (b) of the  $\text{Ca}_2\text{FeReO}_6$  sample as a function of temperature. Dashed lines are guidelines for the eye. Inset: remanence at a temperature range 4–300 K; dashed lines are guidelines for the eye.

value of the Bloch exponent ( $n$ ) is large in comparison with 1.5 for a typical ferromagnet. However, at low temperatures, when only the low-order excitations are taken into account, the ferromagnet spin-wave dispersion spectrum is very similar to that of a perfect ferromagnet. At higher temperatures one should observe the acoustic and optical branches in the dispersion spectra for both magnetic sublayers separately. The unusual behaviour observed as a function of temperature could be associated with the existence of antiferromagnetic correlation due to the Fe–Re coupling.

The coercive field follows the linear dependence with temperature (see upper inset in the figure 4), as expected, and it changes from 0.05 T at 300 K to 0.24 T at 4 K. The remanence is about 50% of the saturation magnetization value and is lowering linearly with increasing temperature.

In the case of the  $\text{Ca}_2\text{FeReO}_6$  some anomalous temperature dependence of the magnetization is visible in the low temperature range below 175 K (see figure 5(a)). The maximum value of the measured magnetization is  $3.12(1) \mu_{\text{B}}/\text{f.u.}$  and is stable in the range of  $0.02 \mu_{\text{B}}/\text{f.u.}$  up to 140 K. Eventually it drops at 180 K to  $3.04 \mu_{\text{B}}/\text{f.u.}$  The latter temperature is reported [40] to be close to the temperature of the structural transition between two monoclinic phases with slightly different lattice parameters and different direction of the spontaneous magnetization axis [10]. In figure 5(b) we plot the coercive field ( $H_{\text{C}}$ ) versus the temperature. It exhibits two linear slopes as a function of temperature. The change of slope occurs at about 130 K, around the structural transition temperature. The maximum value obtained for  $H_{\text{C}}$  is 1.03 T at 4 K. It decreases fast up to 110 K by more than 50% and changes much more slowly from 0.33 T at 140 K to 0.21 T at room temperature. In the latter temperature interval the coercivity follows the normal linear trend as in other double perovskite family materials, not undergoing any magnetostructural transition. It is very likely that the structural transition contributes to the increase of the magnetic anisotropy due to the strong magnetostructural coupling in Re-based double perovskites. Concerning the remanence of  $\text{Ca}_2\text{FeReO}_6$ , a change of the linear slope is visible and the fastest change is occurring between 100 and 175 K (see the inset in figure 5(a)). A colossal magnetoresistance effect around the magnetostructural transition has been disclosed for  $\text{Ca}_2\text{FeReO}_6$  due to the coexistence of high-temperature and low-temperature phases [41].

A relation between the average ionic radius in  $\text{A}_2\text{FeReO}_6$  and the coercive field is visible (see table 1). This increase in  $H_{\text{C}}$  might be attributed to the presence of structural defects (such as antisites, which are common in double perovskites) acting on the magnetic domains as pinning points. However, as explained earlier in the text, x-ray patterns confirm low defect levels in our samples. High coercivity of the uniaxial systems with large magnetocrystalline anisotropy arises from the need of the magnetization to be rotated to the hard axis direction in order to demagnetize the material in contrast to cubic systems with an easy plane. In Re-based double perovskites large magnetic anisotropy is caused by the interplay of the spin-orbit coupling and crystal field effects. Consequently, we would ascribe the  $H_{\text{C}}$  increase to the increase in anisotropy and orbital contribution to the overall magnetic moment [14, 25].

Among the investigated samples  $\text{Sr}_2\text{CrReO}_6$  is the one with the highest Curie temperature ( $T_{\text{C}} = 610$  K). In figure 6 we show the dependence of the magnetic parameters (saturation magnetization, remanence and coercive field) on the temperature. The maximum value of  $H_{\text{C}}$  is obtained at 4 K and is equal 1.29 T, which is higher than those obtained in the  $\text{A}_2\text{FeReO}_6$  compounds. One can observe the lowering of  $H_{\text{C}}$  with the increase in temperature, which apart from the usual decrease due to the thermally assisted magnetization reversal can be caused by the lowering of the crystal symmetry below room temperature (from cubic to tetragonal) as was observed by neutron powder diffraction [13]. As in the case of the Fe-based series, the strong Re orbital moment causes the magnetocrystalline anisotropy to be important. The structural change is contributing to the anisotropy, and, consequently, to the coercivity of the material.

## 5. Conclusions

Summarizing, we have performed a detailed study of the magnetic properties of the Re-based double perovskite series ( $\text{A}_2\text{FeReO}_6$ ,  $\text{Sr}_2\text{CrReO}_6$ ). We have ascribed the lack of saturation under an applied magnetic field as high as 30 T to the influence of magnetically disordered grain boundaries. We have successfully applied the approach to saturation model widely used in spin-glasses with a weak random anisotropy field to the investigated materials. As the electrical transport is strongly dependent on the tunnelling intergrain resistance, the understanding of the effects caused by the magnetic field on these grain boundaries in defect-free samples will

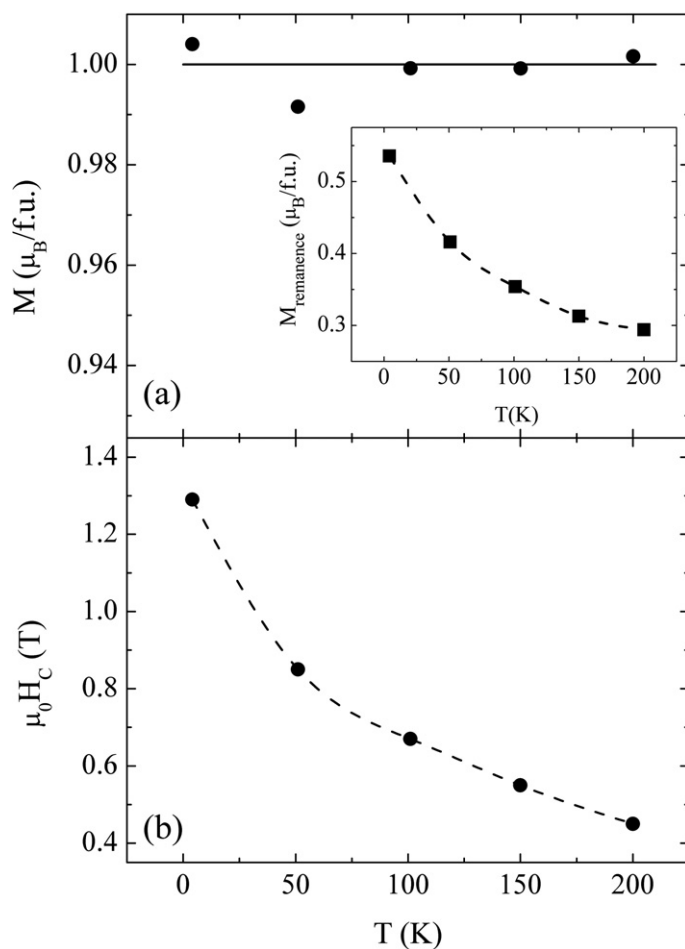


**Figure 6.** Magnetization at 30 T (a) and coercive field (b) of  $\text{Sr}_2\text{CrReO}_6$  sample as a function of temperature. Inset (a): remanence magnetization as a function of temperature. Dashed lines are guides to the eye.

be of great importance. We have also investigated the thermal evolution of the saturation magnetization, remanence and the coercive field. The relation between the coercivity of the material and the magnetocrystalline anisotropy was shown, which has demonstrated the importance of the unquenched Re orbital moment in the magnetism of the Re-based double perovskite family.

### Acknowledgments

Financial support by the Spanish Ministry of Science (through project MAT2005-04562 and MAT2005-05565-C02-02 including FEDER funding), and by the Aragon Regional Government (DGS PIP017) is acknowledged. Part of this work has been supported by EuroMagNET under the EU contract RII3-CT-2004-506239 of the 6th Framework ‘Structuring the European Research Area, Research Infrastructures Action’. We are grateful for the sample synthesis carried out by R Córdoba.

**References**

- [1] Bibes M and Barthelemy A 2007 *IEEE Trans. Electron. Devices* **54** 1003–23
- [2] Kobayashi K-I, Kimura T, Sawada H, Terakura K and Tokura Y 1998 *Nature* **39** 677–80
- [3] Serrate D, De Teresa J M and Ibarra M R 2007 *J. Phys.: Condens. Matter* **19** 023201
- [4] Prellier W, Smolyaninova V, Biswat A, Gelley C, Greene R L, Remesha K and Gopalakrishnan J 2000 *J. Phys.: Condens. Matter* **12** 965–73
- [5] Kato H, Okuda T, Okimoto Y, Tomioka Y, Takenoya Y, Ohkudo A and Kawasaki M 2002 *Appl. Phys. Lett.* **81** 328–30
- [6] Krockenberger Y, Mogare K, Reehuis M, Tovar M, Jansen M, Vaitheeswaran G, Kanchana V, Bultmark F, Delin A, Wilhelm F, Rogalev A, Winkler A and Alff A 2007 *Phys. Rev. B* **75** 020404(R)
- [7] Longo J and Ward R 1961 *J. Am. Chem. Soc.* **83** 2816–8  
Sleight A W, Longo J and Ward R 1962 *Inorg. Chem.* **1** 245–50  
Sleight A W and Weiher J F 1972 *J. Phys. Chem. Solids* **33** 679–87
- [8] Alamelu T, Varadaraju U V, Venkatesan M, Douvalis A P and Coey J M D 2002 *J. Appl. Phys.* **91** 8909–11
- [9] Herrero-Martín J, Subías G, Blasco J, García J and Sánchez M C 2005 *J. Phys.: Condens. Matter* **17** 4963–76  
Azimonte C, Cezar J C, Granado E, Huang Q, Lynn J W, Campoy J C P, Gopalakrishnan J and Ramesha K 2007 *Phys. Rev. Lett* **98** 017204
- [10] Granado E, Huang Q, Lynn J W, Gopalakrishnan J, Greene R L and Ramesha K 2002 *Phys. Rev. B* **66** 064409
- [11] Oikawa K, Kamiyama T, Kato H and Tokura Y 2003 *J. Phys. Soc. Japan* **72** 1411–7
- [12] Serrate D, De Teresa J M, Algarabel P A, Marquina C, Morellon L, Blasco J and Ibarra M R 2005 *J. Magn. Magn. Mater.* **290/291** 843–5
- [13] De Teresa J M, Serrate D, Ritter C, Blasco J, Ibarra M R, Morellon L and Tokarz W 2005 *Phys. Rev. B* **71** 092408
- [14] Sikora M, Kapusta Cz, Borowiec M, Oates C J, Prochazka V, Rybicki D, Zajac D, De Teresa J M, Marquina C and Ibarra M R 2006 *Appl. Phys. Lett.* **89** 062509
- [15] Kato H, Okuda T, Okimoto Y, Tomioka Y, Oikawa K, Kamiyama T and Tokura Y 2002 *Phys. Rev. B* **65** 144404
- [16] De Teresa J M, Michalik J M, Blasco J, Algarabel P A, Ibarra M R, Kapusta C and Zeitler U 2007 *Appl. Phys. Lett.* **90** 252514
- [17] De Teresa J M, Serrate D, Blasco J, Ibarra M R and Morellon L 2004 *Phys. Rev. B* **69** 144401
- [18] Kobayashi K-I, Kimura T, Tomioka Y, Sawada H and Terakura K 1999 *Phys. Rev. B* **59** 11159–62
- [19] De Teresa J M, Serrate D, Blasco J, Ibarra M R and Morellon L 2005 *J. Magn. Magn. Mater.* **290/291** 1043–9
- [20] Serrate D, De Teresa J M, Algarabel P A, Ibarra M R and Galibert J 2005 *Phys. Rev. B* **71** 104409
- [21] Azimonte C, Granado E, Cezar J C, Gopalakrishnan J and Ramesha K 2007 *J. Appl. Phys.* **101** 09H115
- [22] Majewski P, Geprägs S, Sangano O, Opel M, Gross R, Wilhelm F, Rogalev A and Alff L 2005 *Appl. Phys. Lett.* **87** 202503
- [23] Vaitheeswaran G, Kanchana V and Delin A 2005 *Appl. Phys. Lett.* **86** 032513
- [24] Vaitheeswaran G, Kanchana V and Delin A 2006 *J. Phys. Conf. Ser.* **29** 50–3
- [25] Michalik J M, De Teresa J M, Ritter C, Blasco J, Serrate D, Ibarra M R, Kapusta C, Freudenberger J and Kozlova N 2007 *Europhys. Lett.* **78** 17006
- [26] Rodríguez-Carvajal J L and Panetier M A 1987 *ILL Report* 87TR014T
- [27] Woodward P M 1997 *Acta Crystallogr. B* **53** 32
- [28] Balcells L, Navarro J, Bibes M, Roig A, Martínez B and Fontcuberta J 2001 *Appl. Phys. Lett.* **78** 781
- [29] Shanon R D 1976 *Acta Crystallogr. A* **32** 751–67
- [30] Perenboom J A A J, Wiegers S A J, Christianen P C M, Zeitler U and Maan J C 2004 *Physica B* **346/347** 659–62
- [31] Chudnovsky E M, Saslow W M and Serota R A 1986 *Phys. Rev. B* **33** 251–61
- [32] Tejada J, Martínez B, Labarta A and Chudnovsky E M 1991 *Phys. Rev. B* **44** 7698–700
- [33] Chudnovsky E M and Serota R A 1982 *Phys. Rev. B* **26** 2697–9  
Chudnovsky E M 1986 *Phys. Rev. B* **33** 2021–3
- [34] Bloch F 1930 *Z. Phys.* **61** 206
- [35] Dyson F J 1956 *Phys. Rev.* **102** 1217–30
- [36] Lofland S E, Scabarozzi T, Morimoto Y and Xu S 2003 *J. Magn. Magn. Mater.* **260** 181–3
- [37] Zajac D, Sikora M, Prochazka V, Borowiec M, Stępień J, Kapusta Cz, Riedi P C, Marquina C, De Teresa J M and Ibarra M R 2007 *Acta Phys. Pol. A* **111** 797–820
- [38] Solontsov A Z 1995 *J. Magn. Magn. Mater.* **140–144** 215–6
- [39] Pauthenet R 1982 *J. Appl. Phys.* **53** 8187–92
- [40] Westerburg W, Lang O, Ritter C, Felser C, Tremel W and Jakob G 2002 *Solid State Commun.* **122** 201–6
- [41] Serrate D, De Teresa J M, Algarabel P A, Galibert J, Ritter C, Blasco J and Ibarra M R 2007 *Phys. Rev. B* **75** 165109